# Morphological and compositional evolution of tourmaline from nodular granite at Lavičky near Velké Meziříčí, Moldanubicum, Czech Republic

## Vývoj morfologie a složení turmalínů z nodulárního granitu v Lavičkách u Velkého Meziříčí, moldanubikum (Czech summary)

*(5 Figs)*

DAVID BURIÁNEK[1] – MILAN NOVÁK[2]

[1] *Czech Geological Survey, Leitnerova 22, 602 00 Brno*
[2] *Institute of Geological Sciences, Masaryk University, Kotlářská 2, 611 37 Brno*

Several distinct paragenetic, morphological and compositional types of tourmaline were described in the Lavičky nodular granite and associated rocks exposed at the NE margin of the Třebíč durbachite massif. Abundant tourmaline I (schorl, *oxy-schorl*) occurs in quartz-tourmaline nodules and vein-like aggregates; tourmaline II (schorl, *oxy-schorl, fluor-schorl*) forms columnar subhedral crystals and their aggregates in coarse-grained pegmatite; rare, dark grey to greyish brown, fibrous tourmaline III (*oxy-dravite, fluor-dravite*) occurs in late quartz veins. Tourmaline I and II contain small inclusions and veinlets of dravite tourmaline (dravite, *fluor-dravite*, *oxy-dravite*) with very complicated textural relations. They are typical for the Lavičky and were only sporadically found in other localities of nodular granites.
Derivation of exchange vectors was complicated. Tourmaline I exhibits combination of the exchange vectors (AlO) $[R^{2+}(OH)]_{-1}$, $(^{\times}\square Al_2O)$ $[NaR^{2+}{}_2(OH)]_{-1}$ and Mg $Fe_{-1}$. Tourmaline II seems to be characterized by the vector $(^{\times}\square Al_2O)$ $[NaR^{2+}{}_2(OH)]_{-1}$. Tourmaline III shows significant participation of the vector (AlO) $[R^{2+}(OH)]_{-1}$ besides the vectors Mg $Fe_{-1}$ and combination of the vectors (CaO) $[Na(OH)]_{-1}$ and $CaR^{2+}O)$ $[^{\times}\square Al(OH)]_{-1}$. Dravite inclusions and veinlets exhibit the dominant exchange vectors $(CaR^{2+})$ $(NaAl)_{-1}$ and Mg $Fe_{-1}$. All types of tourmaline exhibit high participation of the vector F $(OH)_{-1}$. Tourmaline I and II from nodular granite and pegmatite exhibit very similar chemical compositions and substitution mechanisms relative to those from the other nodular tourmaline granites and primitive granitic pegmatites in the Moldanubicum.

*Key words*: tourmaline, chemical composition, biotite granite, barren pegmatite, quartz vein, Moldanubicum, Czech Republic

## Introduction

Tourmaline is a common mineral in peraluminous granitic rocks (see e.g., London et al. 1996, London 1999 and references therein). It is stable well above the solidus of felsic magmas (e.g., Bénard et al. 1985, London et al. 1996); however, tourmaline may have crystallized as an early magmatic mineral (London – Manning 1995) or as a rather late mineral in a transitional stage from late solidus (magmatic) to early subsolidus (hydrothermal) conditions (see e.g., Sinclair – Richardson 1992, London – Manning 1995). Additionally, tourmaline often originates from hydrothermal fluids in subsolidus within granites and especially in their exocontacts (e.g., London – Manning 1995, Broska et al. 1998, Pivec et al. 1998, Williamson et al. 2000).

Granites with tourmaline concentrated in nodules (nodular tourmaline granite – NTG) are abundant in the Moldanubicum (Buriánek – Novák 2001). They are almost exclusively spatially associated with high-K, *I*-type granitoid (durbachite) plutons. Tourmaline granite from Lavičky represents the largest body of NTG in the eastern part of the Moldanubicum. Origin of distinct tourmaline types, their chemical composition and B-isotopes from Lavičky were studied by Němec (1975), Novák et al. (1997) and Jiang et al. (2003a, b). We described morphological, textural and paragenetic types of tourmaline in the Lavičky granite, their textural and compositional evolution including substitution mechanisms, and discussed their formation in magmatic *versus* hydrothermal stage and in closed *versus* open system.

## Geological setting

Variscan granitic rocks, variable in composition and age, are widespread all over the Moldanubicum. Five genetic groups of the Variscan granitoids were distinguished by Finger et al. (1997): Late Devonian to Early Carboniferous *I*-type granite (ca. 370–340 Ma); early Carboniferous, deformed *S*-type granite/migmatite (ca. 340 Ma); late Visean and early Namurian *S*-type and high-K, *I*-type granitoids – durbachites (ca. 340–310 Ma); post-collisional *I*-type granodiorites and tonalites (ca. 320–290 Ma); late Carboniferous to Perminan *A*-type leucogranites (ca. 300–250 Ma).

Leucocratic tourmaline-bearing granite from Lavičky is exposed at the NE margin of the Třebíč durbachite massif, which yielded age 338–335 Ma (U/Pb zircon) of magmatic crystallization (Kotková et al. 2003). Granite intrudes durbachite and surrounding migmatized biotite-sillimanite paragneisses of the Strážek Moldanubicum (Fig. 1). The dominant rock in the Lavičky body is a leucocratic, fine- to medium-grained, biotite to two-mica granite. Pegmatite dikes and pods, up to 30 cm thick and several m long, are locally present. They exhibit simple internal structure consisting inward of medium- to coarse-grained granitic unit, gradational to the host leucocratic granite, and rare blocky quartz and blocky K-feldspar in

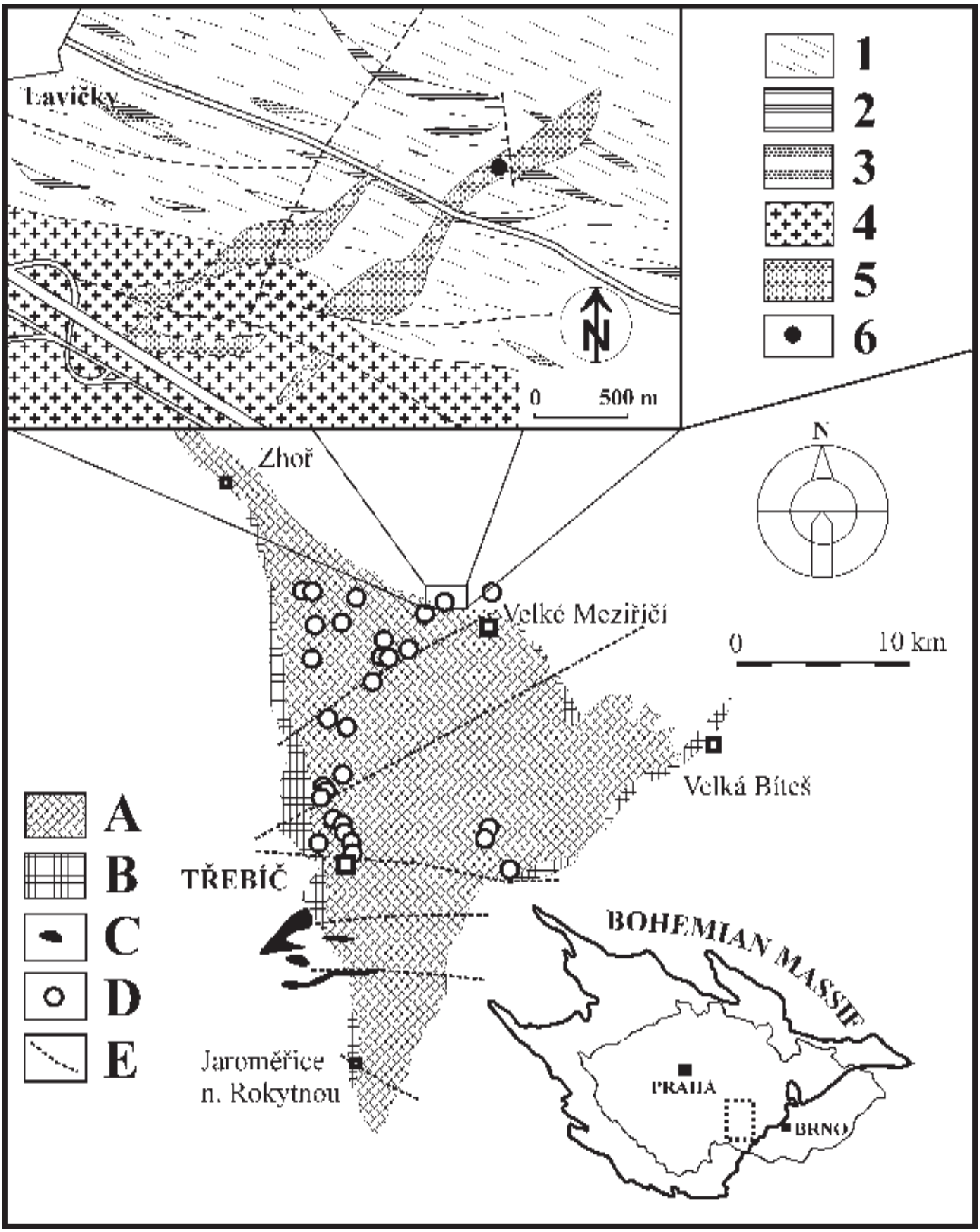


Fig. 1. Geological sketch of the Třebíč durbachite massif with insert simplified geological map of the Lavičky area: A – durbachite; B – biotite granite and migmatite, C – granite with disseminated tourmaline, D – granite with tourmaline concentrated in nodules, E – faults, 1 – migmatite, gneiss; 2 – amphibolite; 3 – pyroxene gneiss; 4 – durbachite; 5 – leucocratic granite; 6 – locality; (modified from Stárková 1990).

centre. Tourmaline occurs dominantly in coarse-grained or blocky unit. Very rare, fracture-filling, hydrothermal quartz veins with rare fibrous tourmaline, up to 2 cm thick, cut granite with sharp contacts and exhibit no apparent hydrothermal alteration of host granite.

## Analytical methods

Electron microprobe analyses of tourmaline and associated minerals were performed on two instruments. (i) Cameca Camebax SX-100, Slovak Geological Survey, Bratislava, Slovakia; wavelength-dispersion mode with a beam diameter of 4–5 μm and an accelerating potential of 15 kV, sample current of 20 nA, counting time 20 s for all elements. The following standards were used ($K_\alpha$ X-ray lines): wollastonite (Si, Ca), albite (Na), chromite (Cr), $Al_2O_3$ (Al), MgO (Mg), $Fe_2O_3$ (Fe), metallic Mn (Mn), $TiO_2$ (Ti), $BaF_2$ (F). (ii) Cameca Camebax SX-50, University of Manitoba, Winnipeg, Canada; wavelength-dispersion mode with a beam diameter of 4–5 μm, an accelerating potential of 15 kV, sample current of 20 nA was used for Si, Al, Ti, Fe, Mn, Mg, Ca, Na and K and current of 40 nA was used for Zn, F and P, counting time 20 seconds for all elements. The following standards were used ($K_\alpha$ X-ray lines): diopside (Si, Ca), kyanite (Al), fayalite (Fe), rutile (Ti), pyrope (Mg), spessartine (Mn), albite (Na), orthoclase (K), fluorapatite (P, F) and gahnite (Zn). The data were reduced on-line using the PAP routine (Pouchou – Pichoir 1984, 1985).

Structural formulae of tourmaline were calculated using the following site assignments and methods. The general tourmaline formula is $X\,Y_3\,Z_6\,T_6\,O_{18}\,(BO_3)_3\,V_3\,W$ where $X$ = Na, Ca, K, vacancy; $Y$ = Fe, Mg, Al, Mn, Zn, Ti; $Z$ = Al, Mg; $T$ = Si, Al; $V$ = O, OH; $W$ = O, OH, F (Hawthorne – Henry 1999). The formula of tourmaline were calculated on the basis $T + Z + Y = 15$, assuming: (i) all Fe is divalent, (ii) B = 3, (iii) no Li is present, (iv) stoichiometric amounts of $H_2O$ as $(OH)^-$, ${}^{W}O + {}^{W}F + {}^{V+W}OH = 4$.

Chemical analyses of granite were carried at the Acme Analytical Laboratories, Vancouver, Canada. Major element contents were determined using ICP ES and trace elements by ICP MS methods.

## Results

### *Petrography*

Fine- to medium-grained biotite to two-mica leucocratic granite typically exhibits a hypidiomorphic texture. The granite has the average modal composition: quartz 32–33, K-feldspar 36–41, plagioclase 22–29 and biotite 1–5 (all in vol. %). Quartz is generally strained, as indicated by the common presence of undulatory extinction. K-feldspar is typically perthitic. Subhedral to euhedral plagioclase ($An_{11–27}$) is commonly homogenous or it sporadically exhibits concentric continuous zoning. Both feldspars especially plagioclase are hydrothermally altered. Small flakes of biotite (annite: $X_{Fe}$ = 0.67–0.73, ${}^{T}Al$ = 2.56–2.62) are locally replaced by chlorite. Subhedral flakes of secondary muscovite commonly replace feldspars. Accessory minerals include euhedral prismatic andalusite, in part replaced by muscovite, cordierite completely replaced by a fine-grained mixture of muscovite and biotite (phlogopite to annite: $X_{Fe}$ = 0.44–0.66, ${}^{T}Al$ = 1.81–2.73), as well as fluorapatite, zircon, monazite and xenotime.

Tourmaline is largely concentrated in nodules and vein-like aggregates, but it is present as a very rare accessory mineral in granite as well. The nodules, up to 15 cm in diameter, or rare vein-like aggregates, up to 4 cm thick and several m long, comprise almost all tourmaline occurring at this locality. The nodules and vein-like aggregates consist of tourmaline 36–40, quartz 42–53, plagioclase 14–6 and K-feldspar 0–6 (all in vol. %). Both nodules and vein-like aggregates are composed of two texturally and compositionally distinct zones. (i) Central zone consists of tourmaline, quartz, variable but subor-

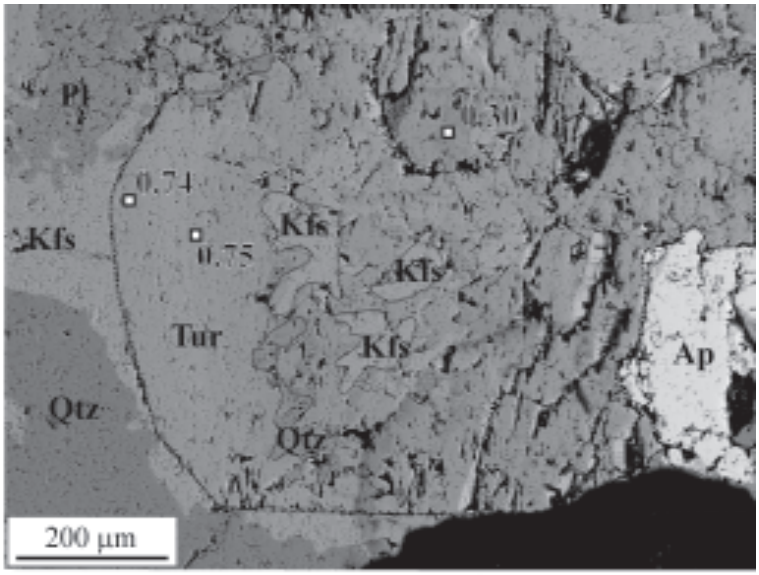


Fig. 2. BSE-image of subhedral tourmaline I replacing K-feldspar. Numbers next to symbols are Fe/(Fe+Mg) ratios. Qtz – quartz, Kfs – K-feldspar, Plg – plagioclase, Ap – apatite.

dinate amount of K-feldspar, plagioclase and fluorapatite. Anhedral to subhedral tourmaline is commonly 0.1 to 2 mm in size; it is typically interstitial between grains of quartz and commonly replaces feldspars (Fig. 2). (ii) Leucocratic halo, 0.5 to 3 cm thick, surrounds each nodule and vein-like aggregate. It is similar in both mineralogy and texture to the adjacent granite except the absence of biotite and commonly finer grain-size.

Pegmatite dikes and pods exhibit simple zoning and mineral assemblage; outer granitic unit: K-feldspar + plagioclase + quartz plus minor biotite + muscovite ± tourmaline, inner blocky unit: K-feldspar + quartz plus minor tourmaline + muscovite. No accessory minerals except abundant apatite and very rare allanite were found in pegmatite. Late hydrothermal quartz veins consist of grey massive quartz with rare, dark greyish brown aggregates of fibrous tourmaline, which may have locally crystallized into open space as hair-like aggregates.

*Geochemistry*

Lavičky granite is leucocratic and slightly metaluminous to peraluminous (A/CNK = 0.99–1.15) with narrow range of $SiO_2$ (74–75 wt.%). The K/Rb ratios range between 241–283, low Rb contents (174–195 ppm) and elevated contents of Sr (144–174 ppm) and Ba (520–552 ppm) are typical. The Lavičky granite is slightly depleted in REE (∑REE = 20–26 ppm) compared to the other NTG (∑REE = 40–86 ppm; Buriánek – Novák 2003). The chondrite-normalized REE patterns are parallel with those of the other NTG patterns and show slight LREE enrichment ($La_N/Lu_N$ = 1.9–2.2) and a positive Eu anomaly (Eu/Eu*= 1.3–1.8). In general, the Lavičky granite has similar geochemical signature as the other NTG in the Moldanubicum except increased $K_2O$ and CaO and decreased $Na_2O$ and Rb (Tab. 1). High $CaO/Na_2O$ ratios are typical for peraluminous granites derived from feldspar-rich psammitic rocks (Sylvester 1998).

Quartz-tourmaline nodules are apparently Fe, Mg and B enriched, with 3.12 to 5.06 wt.% FeO, 0.99 to 1.44 wt.% MgO and 4.26 wt.% $B_2O_3$ (Němec 1975), whereas the host granite contains up to 0.22 to 0.38 wt.% FeO and 0.16 to 0.33 wt.% MgO. The leucocratic halo is slightly Fe, Mg, Ti and K depleted and Na, P and Si enriched relative to granite.

*Tourmaline*

*Description*

Tourmaline occurs in three distinct paragenetic and morphological types in macroscopic scale (cf. Novák et al. 1997). The most abundant black tourmaline I from quartz-tourmaline nodules and vein-like aggregates forms subhedral to anhedral interstitial grains, 0.1 to 2 mm in size. Tourmaline I with khaki-colored pleochroism exhibits locally oscillatory or patchy zoning. Black tourmaline II occurs as columnar subhedral crystals and their aggregates, up to 4 cm long, in coarse-grained or blocky pegmatite.

Table 1. Chemical compositions of rocks in the Lavičky granite: (1–2) granite, (3) nodule and (4) range of chemical compositions of the nodular tourmaline granites from the Třebíč durbachite massif.

| Sample | 1 | 2 | 3 | 4 |
|---|---|---|---|---|
| Rock type | granite | granite | nodule | granite |
| $SiO_2$ | 74.12 | 74.72 | 71.82 | 73.45–74.71 |
| $TiO_2$ | 0.07 | 0.08 | 0.17 | 0.08–0.18 |
| $Al_2O_3$ | 14.22 | 13.71 | 16.26 | 13.62–14.83 |
| $Fe_2O_{3tot}$ | 0.62 | 0.42 | 3.48 | 0.60–1.77 |
| MnO | 0.01 | 0.01 | 0.04 | 0.01–0.05 |
| MgO | 0.19 | 0.16 | 0.99 | 0.13–0.32 |
| CaO | 1.51 | 1.71 | 0.97 | 0.56–0.79 |
| $Na_2O$ | 2.81 | 2.65 | 2.15 | 3.35–3.93 |
| $K_2O$ | 5.67 | 5.91 | 2.77 | 4.26–4.97 |
| $P_2O_5$ | 0.14 | 0.11 | 0.14 | 0.06–0.25 |
| LOI | 0.46 | 0.30 | 1.00 | 0.10–1.00 |
| Total | 99.82 | 99.78 | 99.79 | 99.13–99.95 |
| ppm | | | | |
| Rb | 194 | 174 | 87 | 206–334 |
| Cs | n.d. | 6.0 | 3.1 | 6.0–77.0 |
| Sr | 155 | 174 | 84 | 56–191 |
| Ba | 539 | 538 | 233 | 202–711 |
| Cu | 0.0 | 1.0 | 1.0 | 2.0–6.0 |
| Pb | 27.0 | 6.0 | 3.0 | 9.0–72.0 |
| Zn | 4.0 | 5.0 | 2.0 | 2.0–22.0 |
| Sn | 0.0 | 0.5 | 12.0 | 2.0–32.0 |
| W | 0.0 | 4.0 | 1.0 | 1.0–5.0 |
| Mo | n.d. | <1.0 | <1.0 | 3.0–28.0 |
| Sb | 1.08 | <0.50 | <0.50 | 0.80–0.00 |
| Tl | 0.0 | 0.2 | <0.1 | 0.1–1.3 |
| Ga | 14.0 | 13.2 | 1.9 | 19.7–13.3 |
| Nb | 6.9 | 3.9 | 5.7 | 6.1–15.4 |
| Ta | 0.5 | 1.9 | 3.6 | 1.0–3.6 |
| Zr | 38.7 | 45.4 | 48.8 | 29.4–91.5 |
| Hf | 1.6 | 1.8 | 1.7 | 1.0–3.2 |
| Y | 8.7 | 13.8 | 19.2 | 14.5–24.1 |
| Th | 3.1 | 4.6 | 3.1 | 2.7–16.1 |
| U | 7.0 | 4.2 | 4.7 | 2.1–20.1 |
| La | 3.2 | 3.9 | 7.0 | 6.9–17.1 |
| Ce | 6.3 | 8.4 | 14.1 | 14.6–33.8 |
| Pr | 0.76 | 0.99 | 1.52 | 1.69–3.86 |
| Nd | 3.0 | 3.9 | 5.7 | 6.3–14.2 |
| Sm | 0.9 | 1.1 | 1.7 | 1.5–3.1 |
| Eu | 0.56 | 0.50 | 0.40 | 0.37–0.79 |
| Gd | 0.98 | 1.25 | 1.90 | 1.47–3.00 |
| Tb | 0.20 | 0.27 | 0.39 | 0.33–0.57 |
| Dy | 1.44 | 2.03 | 2.88 | 2.38–4.18 |
| Ho | 0.32 | 0.43 | 0.59 | 0.51–0.88 |
| Er | 0.99 | 1.38 | 2.02 | 1.37–2.58 |
| Tm | 0.16 | 0.22 | 0.32 | 0.17–0.45 |
| Yb | 1.12 | 1.39 | 2.06 | 1.38–3.15 |
| Lu | 0.16 | 0.21 | 0.32 | 0.19–0.18 |

Dark grey to greyish brown, fibrous tourmaline III occurs in hydrothermal quartz veins. Tourmaline III is highly heterogeneous in the BSE image showing locally well-developed but complicated oscillatory zoning.

Tourmaline I and II contain microscopic inclusions and veinlets of dravite composition with very complicated textural relations to the host tourmaline. Inclusions form homogeneous irregular blebs, up to 100 μm in size (Fig. 3a), and narrow heterogeneous zones and blebs, about 5 to 10 μm in size, in oscillatory-zoned tourmaline (Fig. 3b). Their position in the sequence of crystallization is uncertain. Dravite veinlets, up to 10 μm thick, are highly heterogeneous and show complicated textural relations to the

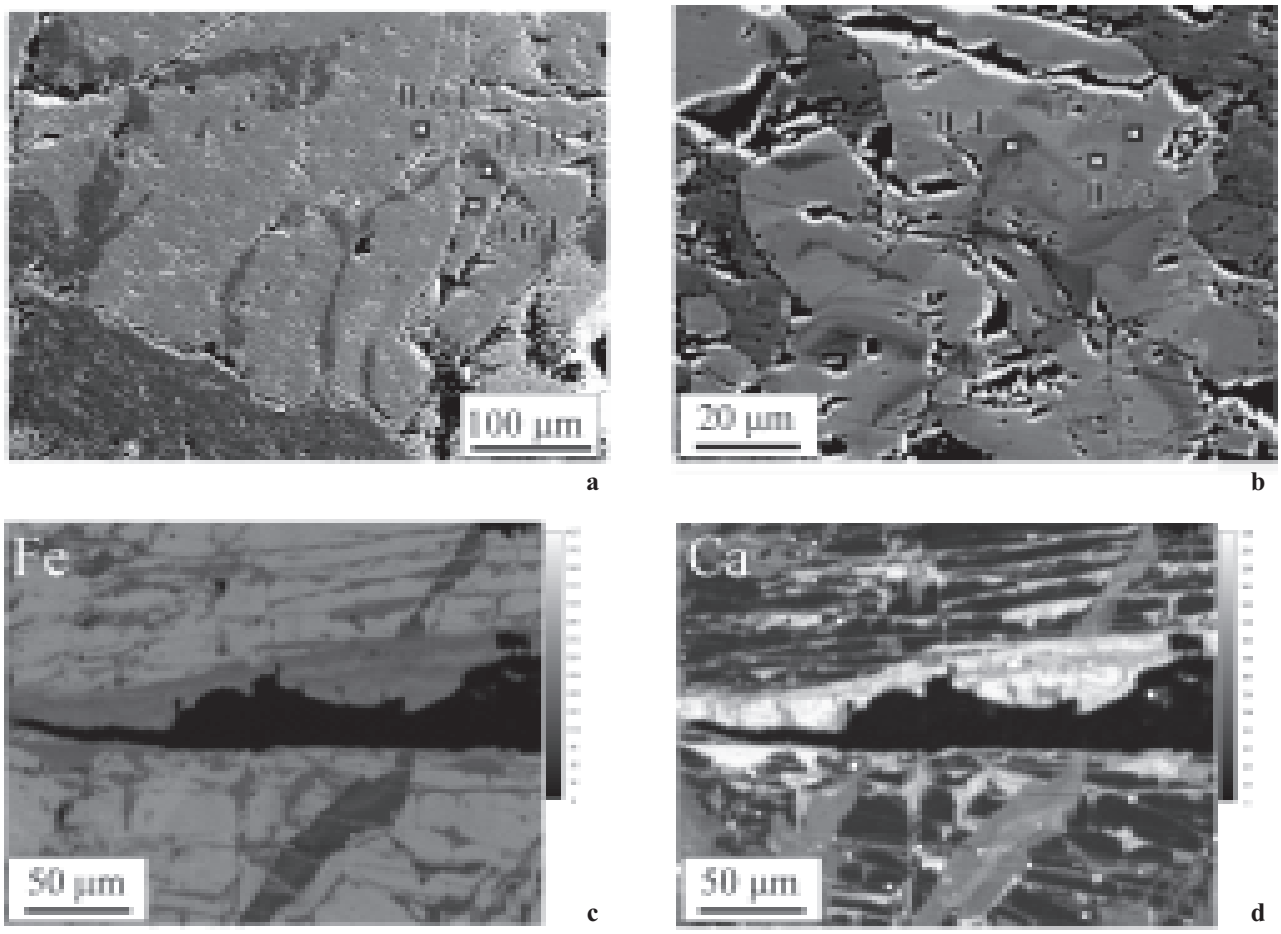


Fig. 3. BSE-image and element distributions in individual textural types of tourmaline; (a) blebs of dravite in tourmaline I; (b) oscillatory-zoned tourmaline I with dravite in cores, (c–d) distributions of Fe and Ca in late dravite veinlets in tourmaline I from vein-like aggregates. Numbers next to symbols are Fe/(Fe+Mg) ratios.

host tourmaline I exclusively from vein-like aggregates. They cut host tourmaline I and earlier dravite inclusions and are apparently late in origin (Fig. 3c, d).

*Chemical composition*

Based on chemical composition and considering textural and paragenetic relationships, three compositionally distinct groups of tourmaline were distinguished. The first group (schorl, *oxy-schorl, fluor-schorl*) is represented by tourmaline I and II, which exhibit similar chemical compositions; the second group involves Mg-rich but commonly Ca-poor tourmaline III (*oxy-dravite, fluor-dravite*) from late hydrothermal quartz veins; the third group involves Mg, Ca-rich tourmaline (dravite, *fluor-dravite, oxy-dravite*) from dravite inclusions and veinlets in tourmaline I and II (Table 2, Fig. 4, 5).

In the first group, the amount of Si in the *T*-site is variable – tourmaline I (5.73 to 5.95) and tourmaline II (5.85 to 6.19; all in *apfu*). The *Z*-site is very likely fully occupied by Al (disregarding possible Mg disorder; cf. e.g., Grice – Ercit 1993). Both tourmaline I and II show Fe > Mg, tourmaline I (0.45 to 1.29) and tourmaline II from pegmatite (0.57 to 0.77; both in *apfu* Mg). The minor cations include low Ti (≥ 0.10 *apfu*) and very low Mn (≥ 0.05 *apfu*). Tourmaline I and II are characterized by moderate to high vacancy in the *X*-site (≥ 0.38 *pfu*) and low to moderate Ca (≥ 0.15 *apfu,* commonly ≥ 0.10 *apfu*, Fig. 4b, 5f), they also exhibit similar F concentrations 0.00 to 0.40 *apfu* F in tourmaline I and 0.27 to 0.46 *apfu* F in tourmaline II (Fig. 4a, 5e, f).

The second group (tourmaline III) shows 5.85 to 6.08 *apfu* Si, the *Z*-site is very likely fully occupied by Al. In the *Y*-site, Mg is dominant with 1.41 to 1.79 *apfu* Mg (Fig. 4b, 5f), the minor cations include low Ti (≥ 0.14 *apfu*) and very low Mn (≥ 0.05 *apfu*). Tourmaline III has low to moderate Ca (≥ 0.18 *apfu*), but mostly ≥ 0.10, and high *X*-site vacancy (≥ 0.41 *pfu*) (see Fig. 4c), it shows variable F concentrations from 0.10 to 0.48 *apfu*.

The third group (dravite inclusions and veinlets) exhibits 5.76 to 6.02 *apfu* Si, only some compositions show $Al_{tot} < 6$, hence Mg possibly enters the *Z*-site (Fig. 4b). Magnesium is dominant in the *Y*-site varying from 1.84 to 2.42 *apfu* Mg in various types of dravite inclusions (Fig. 4b), it is slightly Ti enriched (≥ 0.17 *apfu*). Dravite inclusions and namely veinlets are Ca-enriched (≤ 0.39 *apfu*) and exhibit low *X*-site vacancy (≤ 0.23 *pfu*) relative to the first and second group. The dravite inclusions show highly variable contents of F from 0.00 to 0.71 *apfu*.

Table 2. Representative chemical compositions of tourmaline: (1) tourmaline I, (2) dravite inclusion from tourmaline I, (3) tourmaline II, (4) dravite inclusion from tourmaline II, (5) tourmaline III.

| | 1 | 1 | 2 | 2 | 3 | 3 | 4 | 4 | 5 |
|---|---|---|---|---|---|---|---|---|---|
| $SiO_2$ | 34.60 | 34.20 | 36.60 | 37.13 | 35.10 | 34.60 | 37.20 | 36.80 | 36.00 |
| $TiO_2$ | 0.58 | 0.37 | 0.76 | 0.83 | 0.80 | 0.57 | 0.85 | 0.57 | 1.03 |
| $Al_2O_3$ | 33.40 | 35.00 | 31.00 | 31.67 | 29.90 | 32.10 | 31.50 | 31.20 | 30.50 |
| $B_2O_3$* | 10.15 | 10.24 | 10.62 | 10.76 | 10.05 | 10.09 | 10.68 | 10.57 | 10.33 |
| FeO | 12.00 | 11.30 | 3.63 | 3.30 | 14.70 | 11.90 | 4.62 | 5.46 | 6.80 |
| MnO | 0.16 | 0.13 | 0.04 | 0.02 | 0.25 | 0.16 | 0.00 | 0.01 | 0.00 |
| MgO | 2.01 | 2.05 | 10.00 | 10.04 | 2.23 | 2.75 | 8.94 | 8.51 | 7.21 |
| ZnO | 0.00 | 0.00 | 0.00 | 0.00 | 0.00 | 0.04 | 0.01 | 0.00 | 0.02 |
| CaO | 0.23 | 0.20 | 1.59 | 1.64 | 0.11 | 0.16 | 1.12 | 1.37 | 0.99 |
| $K_2O$ | 0.05 | 0.05 | 0.04 | 0.04 | 0.06 | 0.03 | 0.03 | 0.04 | 0.04 |
| $Na_2O$ | 1.88 | 1.83 | 1.94 | 1.83 | 2.55 | 2.09 | 2.17 | 2.07 | 1.94 |
| $H_2O$* | 2.82 | 3.00 | 2.83 | 2.75 | 2.76 | 2.82 | 3.07 | 3.11 | 2.88 |
| F | 0.55 | 0.37 | 1.13 | 1.36 | 0.85 | 0.52 | 0.44 | 0.30 | 0.65 |
| O=F | –0.23 | –0.16 | –0.48 | –0.57 | –0.36 | –0.22 | –0.19 | –0.13 | –0.27 |
| total | 98.25 | 98.58 | 99.70 | 100.82 | 97.57 | 94.75 | 100.44 | 99.89 | 98.12 |
| | | | | | | | | | |
| Si | 5.927 | 5.807 | 5.988 | 6.000 | 6.067 | 5.962 | 6.055 | 6.048 | 6.055 |
| T-Al | 0.073 | 0.193 | 0.012 | 0.000 | 0.000 | 0.038 | 0.000 | 0.000 | 0.000 |
| B | 3.000 | 3.000 | 3.000 | 3.000 | 3.000 | 3.000 | 3.000 | 3.000 | 3.000 |
| Z-site | | | | | | | | | |
| Al | 6.000 | 6.000 | 5.965 | 6.000 | 6.000 | 6.000 | 6.000 | 6.000 | 6.000 |
| Mg | 0.000 | 0.000 | 0.035 | 0.000 | 0.000 | 0.000 | 0.000 | 0.000 | 0.000 |
| Y-site | | | | | | | | | |
| Ti | 0.075 | 0.047 | 0.094 | 0.101 | 0.104 | 0.074 | 0.104 | 0.070 | 0.130 |
| Al | 0.670 | 0.810 | 0.000 | 0.032 | 0.092 | 0.480 | 0.043 | 0.044 | 0.048 |
| $Fe^{2+}$ | 1.719 | 1.605 | 0.497 | 0.446 | 2.125 | 1.713 | 0.629 | 0.751 | 0.957 |
| Mg | 0.513 | 0.519 | 2.403 | 2.418 | 0.575 | 0.705 | 2.168 | 2.086 | 1.808 |
| Mn | 0.023 | 0.019 | 0.006 | 0.003 | 0.037 | 0.023 | 0.000 | 0.001 | 0.000 |
| Zn | 0.000 | 0.000 | 0.000 | 0.000 | 0.000 | 0.005 | 0.001 | 0.000 | 0.002 |
| ∑ Y | 3.000 | 3.000 | 3.000 | 3.000 | 2.933 | 3.000 | 2.945 | 2.952 | 2.945 |
| X-site | | | | | | | | | |
| Ca | 0.042 | 0.036 | 0.279 | 0.284 | 0.020 | 0.030 | 0.195 | 0.241 | 0.178 |
| Na | 0.624 | 0.602 | 0.615 | 0.573 | 0.855 | 0.698 | 0.685 | 0.660 | 0.633 |
| K | 0.011 | 0.011 | 0.008 | 0.008 | 0.013 | 0.007 | 0.006 | 0.008 | 0.009 |
| Xvac. | 0.323 | 0.351 | 0.098 | 0.135 | 0.112 | 0.265 | 0.114 | 0.091 | 0.180 |
| W-OH | 3.000 | 3.000 | 3.000 | 3.000 | 3.000 | 3.000 | 3.000 | 3.000 | 3.000 |
| V-OH | 0.236 | 0.404 | 0.094 | 0.914 | 0.192 | 0.362 | 0.330 | 0.412 | 0.234 |
| F | 0.298 | 0.199 | 0.585 | 0.695 | 0.465 | 0.283 | 0.227 | 0.156 | 0.346 |
| O | 0.466 | 0.397 | 0.321 | 0.391 | 0.343 | 0.355 | 0.443 | 0.432 | 0.420 |

The third compositional group differs generally in higher Ca, Mg and Ti, in lower Fe, Al, Na and *X*-site vacancy relative to the first group. The second group (tourmaline III from quartz veins) is Mg-rich and Fe-poor, otherwise similar to the first group. Concentrations of F are variable in all groups, the highest concentrations were found in dravite inclusions (third group). Diagram in Fig. 4a indicates high participation of O in the *W*-site in all tourmaline types.

## Discussion and Conclusion

### *Substitution mechanisms in tourmaline*

Derivation of substitution mechanisms in tourmaline from Lavičky is complicated due to scattered data in diagrams (see Fig. 4, 5), which mostly do not allow derivation of simple exchange vectors (cf. Burt 1989) in the individual compositional and textural types of tourmaline.

The plots of analyses of tourmaline I exhibit combination of the exchange vectors (most vectors are derived from the ideal tourmaline composition $NaR^{2+}_3Al_6Si_6O_{18}(BO_3)_3(OH)_3OH$) – $(AlO)[R^{2+}(OH)]_{-1}$, $(^{\times}\square Al_2O)[NaR^{2+}_2(OH)]_{-1}$ and $Mg\,Fe_{-1}$ (Fig. 5a,d). Elevated Ca contents in some analyses indicate participation of some vector involving Ca but its derivation is not possible (see Fig. 5a, b, d). Tourmaline II exhibits the vector $(^{\times}\square Al_2O)[NaR^{2+}_2(OH)]_{-1}$ (Fig. 5a,b), but the data are not too convincing. The substitution mechanisms in tourmaline I and II are similar to those found in primitive barren pegmatites in the Moldanubicum (Novák et al. 2004). Tourmaline III shows significant participation of the vector $(AlO)[R^{2+}(OH)]_{-1}$ besides the vector $Mg\,Fe_{-1}$, and combination of the vectors $(CaO)[Na(OH)]_{-1}$ and $(CaR^{2+}O)[^{\times}\square Al(OH)]_{-1}$. In tourmaline of the third group (dravite inclusions and veinlets) characterized by elevated Ca and low vacancy in the *X*-site the exchange vectors $(CaR^{2+})(NaAl)_{-1}$ and $Mg\,Fe_{-1}$ are dominant, whereas participa-

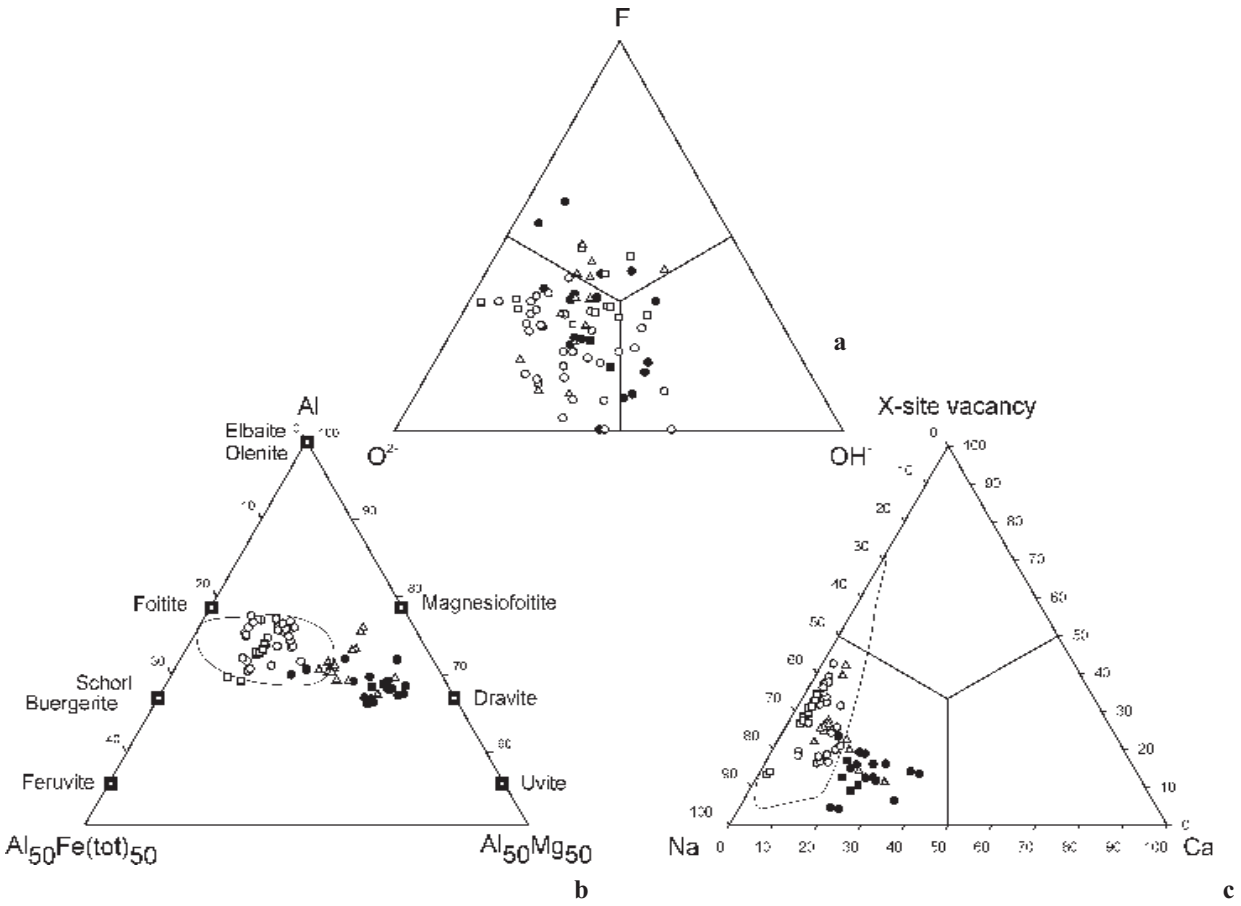


Fig. 4. Composition of tourmaline from Lavičky; (a) $^{W}O$ – OH – F triangle; (b) Fe – Mg – Al triangle; (c) Na+K – Ca – $^{X}\square$ triangle: open circle – tourmaline I; solid circle – dravite inclusions from tourmaline I; open square – tourmaline II, solid square – dravite inclusion in tourmaline II; open triangle – tourmaline III; crosshatch field – tourmaline from other NTG in the Moldanubicum (unpublished data of the authors).

tion of the exchange vector (CaO) $[Na(OH)]_{-1}$ commonly found in Ca, Mg-rich tourmaline (e.g., Henry – Dutrow 1996) seems to be negligible (Fig. 5a). All types of tourmaline exhibit high participation of the vector F $(OH)_{-1}$ (Fig. 5e, f).

*Formation of the distinct morphological and paragentic types of tourmaline in the Lavičky granite*

Tourmaline I (schorl, *oxy-schorl*) from nodules (including vein-like aggregates) sems to be a product of crystallization from highly evolved B-rich and Fe-enriched residual melts and/or fluids during late solidus to subsolidus stage of granite consolidation. Close spatial relations of oval nodules and vein-like aggregates with almost identical textural, paragenetic and compositional features strongly suggest formation of nodules and veins close to the transition between late solidus to early subsolidus conditions. The vein-like aggregates seem to crystallize in solid granite, whereas formation of oval nodules may have started slightly earlier when the host granitic melt likely with large portion of crystals was still in ductile (plastic) state.

Tourmaline II (schorl, *oxy-schorl, fluor-schorl*) from pegmatite exhibits very distinct texture relative to tourmaline I from nodules, but its chemical composition and nature of dravite inclusions are almost identical in both types. The formation of nodules and vein-like aggregates in granite (tourmaline I) and aggregates in pegmatite (tourmaline II) very likely proceeded in similar PTX conditions; however, why they and their host rocks are fairly distinct in texture, grain-size and morphology of crystals, is not clear.

Tourmaline III (*oxy-dravite, fluor-dravite*) from hydrothermal quartz veins is evidently late because these veins fill fractures in solid granite and they are not spatially related to occurrences of tourmaline I and II. Chemical composition of tourmaline III with evidently higher concentrations of Mg (and Ca in some zones) suggests influx of Mg and perhaps Ca from host rocks (metapelite, durbachite).

*Formation of microscopic dravite inclusions and veinlets*

Abundance of microscopic dravite inclusions in tourmaline I and II and dravite veinlets in tourmaline I from vein-like aggregates is a typical feature of tourmalines from Lavičky mentioned already by Novák et al. (1997). However, the dravite inclusions and veinlets display very

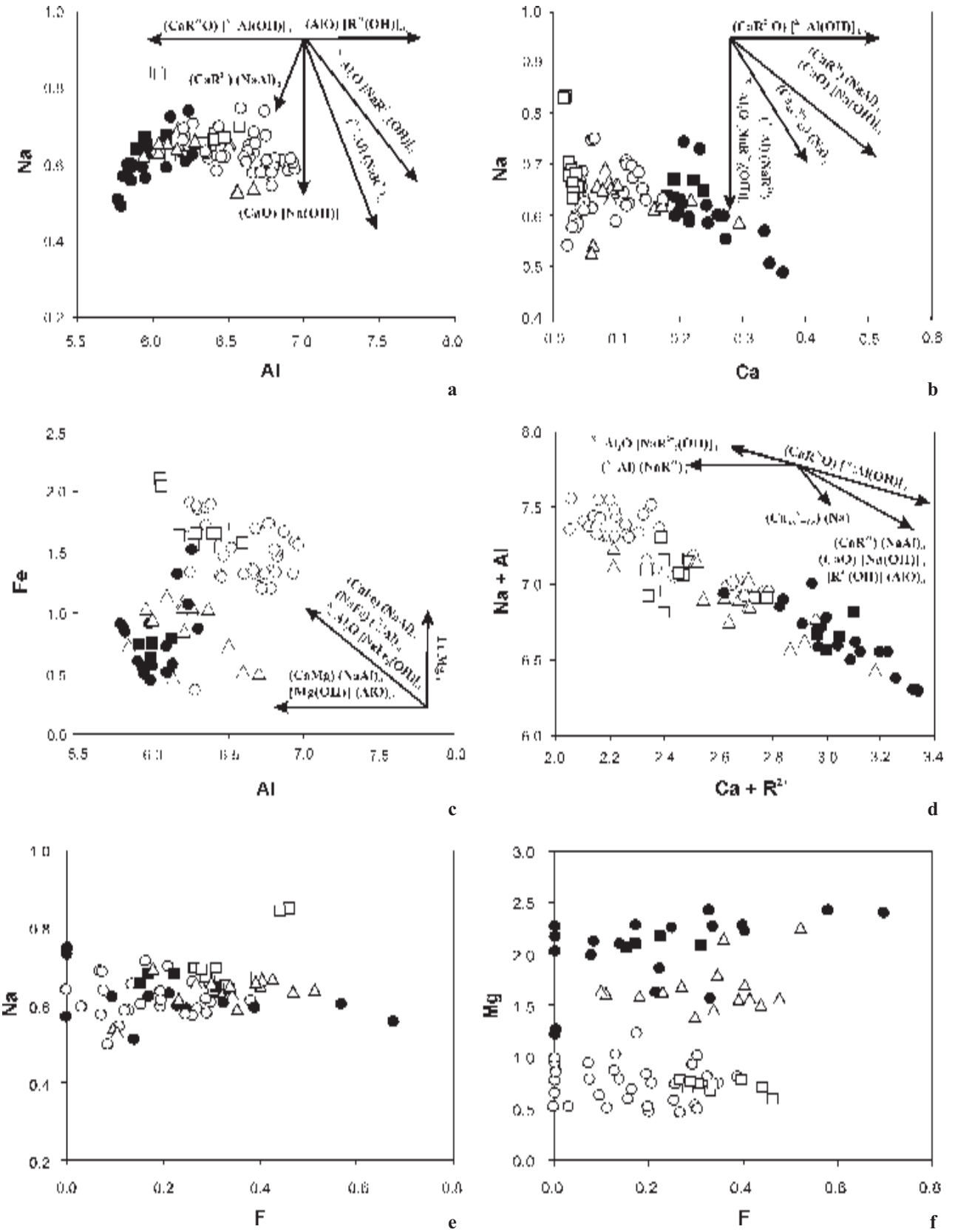


Fig. 5. Composition of tourmaline from Lavičky; (a) Na *versus* Al; (b) Na *versus* Ca; (c) Fe *versus* Al; (d) Na+Al *versus* Ca+$R^{2+}$; (e) Na *versus* F; (f) Mg *versus* F; same symbols as in Fig. 4.

complicated textural relations to host tourmaline and between various types of dravite inclusions and veinlets within a single grain. Homogeneous irregular blebs located in tourmaline I and II (Fig. 3a) and heterogeneous portions in oscillatory zoned tourmaline I (Fig. 3b) have uncertain position in the sequence of crystallization; nevertheless, they are considered to crystallize earlier than thin and highly heterogeneous dravite veinlets from tourmaline I (Fig. 3c, d). Saturation of dravite-rich tourmaline occurred in at least three distinct stages (early dravite inclusions in tourmaline I and II, late dravite veinlets in tourmaline I and fibrous tourmaline III from hydrothermal quartz veins). It may be explained by multistage opening of the Lavičky granite system to metamorphic fluids from host rocks and quartz veins with fibrous tourmaline III may represent the final stage of such mixing. However, the early dravite inclusions may have formed in the system closed to the host rocks. We propose potential explanations of textural and chemical features of these early dravite inclusions as it follows (Fig. 3a, b). (i) The inclusions are relics of early tourmaline, which crystallized in earlier magmatic stage relative to tourmaline I and II. The source of Ca, Mg and Ti was a less fractionated granitic melt. (ii) They are products of early hydrothermal alteration in the system closed to the host rocks (metapelites, durbachites); the sources of Ca, Mg and Ti are probably altered minerals – plagioclase (Ca), cordierite (Mg) and biotite (Mg, Ti). (iii) The inclusions are products of late hydrothermal alteration in the system open to the host rocks (metapelites, durbachites) but still earlier then formation of thin dravite veinlets (Fig. 3c, d); the host rocks are suitable source of Ca, Mg and Ti. None of the above explanations of dravite inclusions is sufficiently supported by textural evidences; nevertheless, the (ii) explanation seems to be most likely. The fine oscillatory zoning in the fibrous tourmaline III may also suggest compositional fluctuation in the hydrothermal fluids, which is typical for hydrothermal tourmaline (e.g., Morgan – London 1987, London – Manning 1995, Dutrow – Henry 2000).

### *Comparison of tourmaline composition with granitic rocks in the Moldanubicum*

Tourmaline I and II from nodular granite and pegmatite exhibit very similar chemical compositions (Fig. 4) and substitution mechanisms relative to those from the other NTG in Moldanubicum (Buriánek – Novák 2001) and in primitive granitic pegmatites of this region (Novák et al. 2004). Similarly, composition of hydrothermal tourmaline III from quartz veins is comparable with related hydrothermal tourmalines in this region (see e.g., Houzar et al. 1998, Pivec et al. 1998). General compositional trends of tourmaline from the quartz-tourmaline nodules in leucocratic granite and from simple barren pegmatite at Lavičky exhibit characteristics typical for tourmaline from Li-poor pegmatites and granites (e.g., Povondra 1981, Manning 1982, Henry – Guidotti 1985, Povondra et al. 1987). However, the Lavičky granite is evidently more primitive than most other nodular granite localities (e.g., Seagull batholith, Yukon; Sinclair – Richardson 1992).

*Acknowledgements.* The authors thank P. Uher and S. Vrána for constructive criticism that significantly improved the manuscript. The work was supported by Granting Agency of the Czech Republic, Grants No. 205/99/0434 and 205/03/0400 to MN and the research project CEZ: J07/98: 143100003.

*Submitted August 5, 2003*

**References**

*Bénard, F. – Moutou, P. – Pichavant, M.* (1985): Phase relations of tourmaline leucogranites and the significance of tourmaline in silicic magmas. – J. Geol., 93: 271–291.

*Broska, I. – Uher, P. – Lipka, J.* (1998): Brown and blue schorl from the Spiš-Gemer granite, Slovakia: composition and genetic relations. – J. Czech Geol. Soc., 43: 1–4, 9–16.

*Buriánek, D. – Novák, M.* (2001): Tourmaline-bearing leucogranites from the Moldanubicum. – Mittl. Österr. Miner. Ges.- 146: 51–53.

– (2003): Tourmaline orbicules in leucogranites as indicator of geochemical fractionation of late solidus to early subsolidus magmatic fluids. – J. Czech Geol. Soc., 48: 1–2, 30.

*Burt, D. M.* (1989): Vector representation of tourmaline composition. – Am. Mineral., 74: 826–839.

*Dutrow, B. L. – Henry, D. J.* (2000): Complexly zoned fibrous tourmaline, Cruzeiro mine, Minas Gerais, Brazil: a record of evolving magmatic and hydrothermal fluids. – Can. Mineral., 38: 131–143.

*Finger, F. – Roberts, M. P. – Haunschmid, B. – Schermair, A. – Steyrer, H. P.* (1997): Variscan granitoids of central Europe: their typology, potential sources and tectonotherm relations. – Mineral. Petrol., 61: 67–96.

*Grice, J. D. – Ercit, T. S.* (1993): Ordering of Fe and Mg in the tourmaline crystal structure: correct formula. – N. Jb. Mineral. Abh., 165: 245–266.

*Hawthorne, F. C. – Henry, D. J.* (1999): Classification of the minerals of the tourmaline group. – Eur. J. Mineral., 11: 201–215.

*Henry, D. J. – Dutrow, B. L.* (1996): Metamorphic tourmaline and its petrologic applications. *In:* Boron: Mineralogy, Petrology and Geochemistry (Grew, E. S. & Anovitz, L. M. eds). Rev. Mineral., 33: 503–557.

*Henry, D. J. – Guidotti, C. V.* (1985): Tourmaline as a petrogenetic indicator mineral: an example from the staurolite-grade metapelites of NW Maine. – Am. Mineral., 70: 1–15.

*Houzar, S. – Novák, M. – Selway, J. B.* (1998): Compositional variation in tourmaline from tourmalinite and quartz segregations at Pernštejn near Nedvědice (Svratka Unit, western Moravia), Czech Republic. – J. Czech Geol. Soc., 43: 53–58.

*Jiang, S. Y. – Buriánek, D. – Novák, M.* (2003a): Locality No. 7: Lavičky near Velké Meziříčí; Nodular tourmaline granite, barren pegmatite, quartz vein. – Field Trip Guidebook, LERM 2003, Nové Město na Moravě, June 2003, 53–60.

*Jiang, S. Y. – Yang, J. H. – Novák, M. – Selway, J.B.* (2003b): Chemical and boron isotopic compositions of tourmaline from the Lavičky leucogranite, Czech Republic. – Geochemical Journ., 37, 545–556.

*Kotková, J. – Schaltegger, U. – Leichmann, J.* (2003): 338–335 Ma old intrusions in the E Bohemian massif – a relic of the orogen-wide durbachitic magmatism in Europian Variscides. – J. Czech Geol. Soc., 48: 80–81.

*London, D.* (1999): Stability of tourmaline in peraluminous granite systems: the boron cycle from anatexis to hydrothermal aureole. – Eur. J. Mineral., 11: 253–262.

*London, D. – Manning, D. A. C.* (1995): Chemical Variation and Significance of Tourmaline from Southwest England. – Econ. Geol., 90: 495–519.

*London, D. – Morgan, G. B. VI – Wolf, M. B.* (1996): Boron in granitic rocks and their contact aureoles. – *In:* Boron: Mineralogy, Petrology

and Geochemistry (Grew, E. S. – Anovitz, L. M. eds). Rev. Mineral., 33: 299–330.

*Manning, D. A. C.* (1982): Chemical and morphological variation in tourmalines from the Hub Kapong batholith of peninsular Thailand. – Mineral. Mag., 45: 139–147.

*Morgan, G. B. VI – London, D.* (1987): Alteration of amphibolitic wallrocks around the Tanco rare-element pegmatite, Manitoba. – Am. Mineral., 72: 1097–1121.

*Němec, D.* (1975): Genesis of tourmaline spots in leucocratic granites. – N. Jb. Mineral. Mh., 7: 308–317.

*Novák, M. – Povondra, P. – Selway, J. B.* (2003): Schorl-*oxy-schorl* to dravite–*oxy-dravite* tourmaline from granitic pegmatites; examples from the Moldanubicum, Czech Republic. – Eur. J. Mineral., accepted.

*Novák, M. – Selway, J. B. – Uher, P.* (1997): Locality No. 6: Lavičky near Velké Meziříčí, quartz-tourmaline orbicules in leucocratic two-mica granite tourmaline in barren pegmatite and hydrothermal quartz-tourmaline veins. – Field Trip Guidebook, International Symposium Tourmaline 1997, Nové Město na Moravě, June 1997, 77–84.

*Pivec, E. – Štemprok, M. – Novák, J. K. – Lang, M.* (1998): Tourmaline as a late-magmatic or postmagmatic mineral in granites of the Czech part of the Krušné hory – Erzgebirge batholith and its contact zone. – J. Czech Geol. Soc., 43: 17–23.

*Pouchou, J. L. – Pichoir, F.* (1984): A new model for quantitative analysis. I. Application to the analysis of homogeneous samples. – La Recherche Aérosp., 3: 13–38.

– (1985): "PAP" procedure for improved quantitative microanalysis. – Microbeam Anal., 20: 104–105.

*Povondra, P.* (1981): The crystal chemistry of tourmalines of the schorl-dravite series. – Acta Univ. Carol., Geol., 3: 223–264.

*Povondra, P. – Pivec, E. – Čech, F. – Lang, M. – Novák, F. – Prachař, I. – Ulrych, J.* (1987): Přibyslavice peraluminous granite. – Acta Univ. Carol., Geol., 3: 183–283.

*Sinclair, W. D. – Richardson, J. M.* (1992): Quartz-tourmaline orbicules in the Seagull batholith, Yukon Territory. – Can. Mineral., 30: 923–935.

*Stárková, I.* (1990): Geologická mapa ČR 1:50 000, list 23–24 Polná.– Ústř. Úst. Geol., Praha.

*Sylvester, P. J.* (1998): Post-collisional strongly peraluminous granites. – Lithos, 45: 29–44.

*Williamson, B. J. – Spratt, J. – Adams, J. T. – Tindle, A. G. – Stanley, C. J.* (2000): Geochemical constraints from tourmaline hydrothermal overgrowths on the evolution of mineralising fluids in southwest England. – J. Petrol., 41: 1439–1453.

## Vývoj morfologie a složení turmalínů z nodulárního granitu v Lavičkách u Velkého Meziříčí, moldanubikum

V nodulárním granitu z Laviček bylo popsáno několik parageneticky a morfologických typů turmalínu lišících se chemickým složením. Hojný černý turmalín I (skoryl, *oxy-skoryl*) se vyskytuje v křemen-turmalínových nodulích a žilných agregátech v granitu. Černý turmalín II (skoryl, *oxy-skoryl, fluor-skoryl*) tvoří sloupcovité, nedokonale vyvinuté krystaly a jejich agregáty v hrubě zrnitém pegmatitu. Vzácné tmavě šedé až šedohnědé vláknité agregáty turmalínu III (dravit, *oxy-dravit, fluor-dravit*) se vyskytují na pozdních křemenných žilách. Turmalín I a II obsahují časté inkluze a žilky mladšího dravitu (*fluor-dravit*, *oxy-dravit*) s velmi komplikovaným texturními vztahy.

Odvození substitučních mechanismů je komplikované. V turmalínu I se uplatňují především vektory (AlO) $[R^{2+}(OH)]_{-1}$, $(^{\times}\square Al_2O)$ $[NaR^{2+}{}_2(OH)]_{-1}$ and Mg $Fe_{-1}$, v turmalínu II se zdá být dominantní vektor $(^{\times}\square Al_2O)$ $[NaR^{2+}{}_2(OH)]_{-1.}$ V turmalínu III byly zjištěny vedle dominantního vektoru (AlO) $[R^{2+}(OH)]_{-1}$ také vektor Mg $Fe_{-1}$ a kombinace vektorů (CaO) $[Na(OH)]_{-1}$ a $(CaR^{2+}O)$ $[^{\times}\square Al(OH)]_{-1}$. Dravitové inkluze a mladší žilky ukazují na hlavní vektory $(CaR^{2+})(NaAl)_{-1}$ a Mg $Fe_{-1}$, zatímco vektor (CaO) $[Na(OH)]_{-1}$ je asi zanedbatelný. Všechny typy turmalínu ukazují na výrazné uplatnění vektoru F $(OH)_{-1}$. Turmalín I a II z noduláního granitu a pegmatitu mají velmi podobné chemické složení a substituční mechanismy jako turmalíny z jiných nodulárních turmalinických granitů a primitivních Li-chudých granitických pegmatitů v moldanubiku.